Liquid Crystal Poly(glycidyl ether)s by Anionic Polymerization and Polymer-Analogous Reaction

Maria Chiara BIGNOZZI, Sante A. ANGELONI,* Michele LAUS,*
Luca INCICCO,* Oriano FRANCESCANGELI,** Dietmar WOLFF,***
Giancarlo GALLI,**** and Emo CHIELLINI****

*Dipartimento di Chimica Applicata e Scienza dei Materiali,
Viale Risorgimento 2, 40136 Bologna, Italy*
** Dipartimento di Chimica Industriale e dei Materiali,
Viale Risorgimento 4, 40136 Bologna, Italy*
*** Dipartimento di Scienze dei Materiali e della Terra, and Istituto Nazionale per la Fisica della
Materia, Via Brecce Bianche, 60131 Ancona, Italy*
**** Technische Universität Berlin, Institut für Technische Chemie,
Straße des 17. Juni 135, 10623 Berlin, Germany*
***** Dipartimento di Chimica e Chimica Industriale,
Via Risorgimento 35, 56126 Pisa, Italy*

ABSTRACT: Two new series of liquid crystalline poly(glycidyl ether)s I and II containing a side-chain 4-alkoxy-azobenzene mesogenic unit were prepared according to two different synthetic routes. The former were prepared by ring-opening anionic polymerization of different mesogenic epoxides, while the latter were prepared by grafting the same mesogenic side chain onto preformed poly(epichlorohydrin) to different substitution extents. Poly(glycidyl ether)s I formed a sequence of different smectic mesophases and nematic mesophases, depending on the length of the alkoxy tail. For poly(glycidyl ether)s II the kind of the phase behavior (not liquid crystalline, nematic, nematic and smectic) was strongly correlated with the extent of mesogenic side-chain incorporation with greater degrees of substitution favoring the onset of more stable and ordered mesophases. No smectic monolayer arrangement was observed, but only bilayer smectic structures, either S_{A2} or S_{C2}, were detected by X-ray diffraction investigations on powder or magnetically aligned samples.
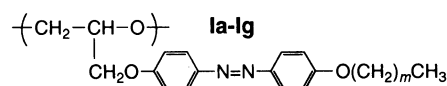KEY WORDS   Poly(glycidyl ether) / Anionic Polymerization / Polymer-Analogous Reaction / Liquid Crystal / Bilayer Smectic /

The synthesis and characterization of side-chain liquid crystalline (LC) polymers, most of which are poly-acrylates, polymethacrylates, or polysiloxanes, have greatly evolved in the last years.[1] The phase behavior is known to depend upon several parameters such as the structure of the polymer backbone, the mesogenic unit and the nature and the length of flexible spacer connecting the mesogenic group to the polymer backbone.

As a general statement, it is usually reported that the flexible spacer connecting the mesogenic unit to the polymer backbone must decouple the dynamics of the backbone from that of the mesogenic side groups. In fact, most polymers with mesogenic group directly attached to the backbone do not show LC behavior.[2,3] However, LC behavior has recently been observed in poly(glycidyl ether)s whose side groups are directly attached to the polymeric backbone.[4-7] It was claimed that when the driving force toward side-chain ordering is sufficiently strong to overcome the energetic constraints associated with the distortion of the polymer chain from the random coil conformation, the polymer can exhibit LC mesophases. In this respect, poly(glycidyl ether)s are particularly attracting because of the inherently high flexibility of the poly(oxyethylene) backbone. In addition, they can be prepared following at least two different synthetic routes, that is by i) ring-opening polymerization of a mesogenic epoxide, and ii) polymer-analogous reaction starting from the appropriate preformed polymeric matrix. As the materials prepared by different methods should differ in terms of molar mass, molar

mass distribution, structural regularity and tacticity, it would be possible to prepare polymers with the same basic composition but with different LC behavior.

To elucidate this point, in the present work we investigated the synthesis and the LC behavior of new side-chain LC poly(glycidyl ether)s prepared according to two different approaches. Poly(glycidyl ether)s **Ia**—**Ig** were prepared *via* anionic ring-opening polymerization of various 4-alkoxy-4'-(2,3-epoxy-propoxy)azobenzenes in which the length of the terminal alkoxy tail increased from $m=0$ to $m=9$. Poly(glycidyl ether)s **IIb(1)**—**IIb(7)** ($m=1$), based on the same mesogenic repeat unit as

m	0	1	2	3	4	5	9
I	a	b	c	d	e	f	g
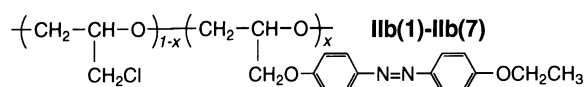
x	0.24	0.40	0.55	0.70	0.73	0.75	0.80
IIb	(1)	(2)	(3)	(4)	(5)	(6)	(7)

Chart 1.

polymer **Ib**, were obtained, *via* a polymer-analogous reaction by grafting the mesogenic 4-hydroxy-4'-ethoxy-azobenzene onto commercial poly(epichlorohydrin) to different extents. It was in fact anticipated that the LC behavior of the polymer samples would be influenced by their molar mass, the main chain stereoregularity, the length of the 4-alkoxy group and the degree of substitution.

EXPERIMENTAL

Materials

Epichlorohydrin (**1**) (Aldrich) was distilled just before use (28—30°C/100 mmHg). Poly(epichlorohydrin) (**4**) (Aldrich) was used as received. 4-Hydroxy-4'-alkoxy-azobenzenes (**2a**—**2g**) were synthesized according to literature.[8] *t*-Butyl alcohol was dried on anhydrous sodium sulfate and then distilled, under dry argon, over calcium hydride immediately before use. Potassium *t*-butoxide was obtained by a literature method[9] and then crystallized from tetrahydrofuran. The potassium *t*-butoxide concentration in tetrahydrofuran solution was determined by titration with sulfuric acid, using phenolphthalein as the indicator. Commercial 18-crown-6 (Aldrich) was dissolved in anhydrous acetonitrile to precipitate as acetonitrile complex, which was filtered and heated to 70°C under vacuum to give the dry 18-crown-6.[10]

4-Methoxy-4'-(2,3-epoxy-propoxy)azobenzene (**3a**)

A mixture of 7.9 g (34.6 mmol) of **2a**, 9.6 g (103.7 mmol) of epichlorohydrin (**1**), 1.0 g of benzyltributylammonium bromide and 14.3 g (103.7 mmol) of anhydrous potassium carbonate in 100 mL of 2-butanone was heated to reflux under stirring. After 3 h, the mixture was poured into 100 mL of cold 1.0 M NaOH. The precipitate was filtered and washed with 4 × 100 mL of water and purified by extraction with boiling methanol in a Kumagawa extractor. The solution was evaporated to dryness and the solid residue was crystallized from *n*-propanol with a yield of 60% (mp 126°C). The compound was further purified by column chromatography on silica gel, with dichloromethane as the eluent. Care was taken to avoid exposure to light.

^{1}H NMR (CDCl$_3$, ppm): $\delta = 2.8$—2.9 (2dd, 2H, O–CH_2–CH–); 3.4 (m, 1H, O–CH$_2$–CH); 3.9 (s, 3H, OCH_3); 4.1—4.3 (2dd, 2H, CH_2O–Ph); 7.0 (dd, 4H, arom.); 7.9 (dd, 4H, arom.).

The **3b**—**3g** samples were synthesized following the same procedure with yields ranging from 55 to 70%.

Anionic Polymerization Procedure

The anionic polymerizations were carried out under dry argon that passed over silica gel, molecular sieves and calcium sulfate. The polymerization glassware and the vacuum line were dried in an oven at 200°C before running each polymerization. Tetrahydrofuran was stored on potassium hydroxide and distilled over potassium/benzophenone under dry argon just before use. The monomer was dissolved in 10 mL of anhydrous tetrahydrofuran (initial concentration [M$_0$] = 0.13—0.23 mol L^{-1}) and introduced under argon into a Schlenk tube with the appropriate amount of the initiating system

consisting of a tetrahydrofuran equimolar solution of crown ether and potassium *t*-butoxide. Polymers **Ia**—**Ic** and **Ie**—**Ig** were synthesized starting from the corresponding monomers **3a**—**3c** and **3e**—**3g** with a monomer/initiator molar ratio R ($R = $[M$_0$]/[I$_0$]) equal to 20. Four polymer samples **Id(1)**—**Id(4)** were prepared by varying the ratio of monomer **3d** over initiator, as follows: $R = 5$, **Id(1)**; $R = 10$, **Id(2)**; $R = 20$, **Id(3)**; $R = 30$, **Id(4)**. The polymerizations were conducted in the dark at 25°C for 12 h, after which they were stopped by adding several drops of dilute acetic acid. The reaction mixture was concentrated to small volume and the polymer was precipitated into a large excess of methanol. It was then purified by extraction with boiling methanol in a Kumagawa extractor followed by repeated precipitations from chloroform solutions into methanol. The concentration data and yields are collected in Table I.

Polymer-Analogous Reaction Procedure

1.0 g (10.8 mmol r.u.) of poly(epichlorohydrin) (**4**) in 180 mL of anhydrous dimethyl sulfoxide were heated to 70°C under stirring until complete dissolution. Then 8.0 g (33.1 mmol) of 4-hydroxy-4'-ethoxy-azobenzene (**2b**), 6.0 g (43.4 mmol) of anhydrous potassium carbonate and 0.5 g of benzyltributylammonium bromide were added to the solution. Portions of the reaction mixture were taken out at different times and poured into methanol as follows: **IIb(1)** at 14 h, **IIb(2)** at 24 h, **IIb(3)** at 38 h, **IIb(4)** at 62 h, **IIb(5)** at 72 h, **IIb(6)** at 95 h. After 130 h, the residual mixture was poured into 200 mL of methanol thus leading to sample **IIb(7)**. After precipitation, each sample was filtered and washed with 2 × 50 mL of 0.5 M NaOH, 2 × 50 mL of water and 2 × 50 mL of methanol, and finally dried under vacuum at 60°C for 24 h. The chlorine substitution degree, as evaluated by ^{1}H NMR, ranged from 24% (sample **IIb(1)**) to 80% (sample **IIb(7)**) (Table II).

Characterization

^{1}H and ^{13}C NMR spectra were recorded on a Varian Gemini 200 spectrometer. Number average molar masses were determined by SEC of chloroform solutions with a 590 Waters chromatograph equipped with a Perkin Elmer UV detector using PL gel 10^3 Å or 10^5 Å columns and a Waters U6K injector. Polystyrene standard samples were used for the calibration. Differential scanning calorimetry (DSC) analyses were carried out with a Perkin-Elmer DSC 7. The transition temperatures were taken from the DSC traces of samples annealed by cooling from the isotropic melt, as corresponding to the maximum temperature and to the onset temperature of the enthalpic peaks for polymers and low molar mass samples, respectively, at a scanning rate of 10 K min^{-1}. Optical microscopy observations were performed on polymer films between glass slides by means of a Reichert Polyvar microscope equipped with a programmable Mettler FP52 heating stage at a scanning rate of 10 K min^{-1}.
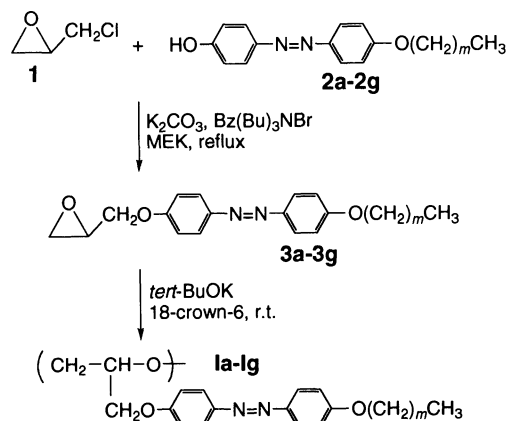
X-Ray diffraction measurements on powder samples were performed using the INEL CPS 120 powder diffractometer, equipped with a position sensitive detector covering 120° in the scattering angle 2θ, with an angular resolution of 0.018° in θ. Ge-monochromatiz-

914

Polym. J., Vol. 31, No. 11-I, 1999

ed Cu-K_α radiation, collimated with an appropriate system of slits, was used. X-Ray diffraction measurements on samples oriented in a magnetic field were carried out in a custom-made, temperature controlled vacuum chamber with a flat film camera at a distance of 84 mm from the sample. Ni-filtered Cu-K_α radiation was used. The samples were oriented inside the chamber by cooling at $0.4\,K\,h^{-1}$ from the isotropic state to the selected temperature under a magnetic field (2.4 tesla) perpendicular to the incident beam. During all the X-ray experiments the temperature of the sample was controlled within 0.1°C.

RESULTS AND DISCUSSION

Synthesis

4-Alkoxy-4'-(2,3-epoxy-propoxy)azobenzene monomers **3a—3g** were synthesized by reacting the corresponding 4-hydroxy-4'-alkoxy-azobenzene (**2a—2g**) with epichlorohydrin (**1**) in the presence of benzyltributylammonium bromide and dry potassium carbonate in 2-butanone (Scheme 1).

Polymers **Ia—Ig** were synthesized by ring-opening polymerization of **3a—3g**, with potassium *t*-butoxide/18-crown-6 ether (1 : 1 mol) as the initiator[10,11] (Scheme 1). Polymers **Ia—Ic** and **Ie—Ig** were synthesized using the same molar monomer/initiator ratio R ($R = [M_0]/[I_0]$) equal to 20, whereas four polymer samples **Id** were prepared with $R = 5$, 10, 20, or 30, thus yielding samples **Id(1)**, **Id(2)**, **Id(3)**, and **Id(4)** respectively. The polymerization yields were low-to-moderate because of incomplete (25—60%) conversion of the monomers. The structure of poly(glycidyl ether)s **Ia—Ig** was determined by ^1H and ^{13}C NMR spectroscopy. The ^{13}C NMR spectrum of sample **Id(4)** is reported, together with relevant assignments, in Figure 1 as a typical example. Assignments of the various signals were made by DEPT and comparison with the spectra of the monomers.

The resonance signals of the carbon atoms of the polymer backbone were detected in the spectral region between 70 and 80 ppm (Figure 2). The C-3 signal was split into two components at 70.5 and 71.6 ppm, because of the different tacticity sequences generated by the presence of an asymmetric carbon atom in the repeat unit. A content of about 70% of dyads r was evaluated for each polymer sample, which was therefore essentially syndiotactic.[12] The resonance signal of the methyl groups of the *t*-butoxide terminal group was also detected in both the ^1H and ^{13}C NMR spectra (see C-1 in Figure 1). Its intensity gradually decreased in going from **Id(1)** to **Id(4)**.

The number average molar mass (M_n) values of the polymers **Ia—Ig**, as estimated by size exclusion chromatography (SEC), ranged from 3500 to 5700 and the first polydispersity index (M_w/M_n) was comprised between 1.10 and 1.15 (Table I). Values of M_n in the range 5000 to 15000 were evaluated by ^1H NMR considering the content of the *t*-butoxide terminal groups. Polymers **Id(1)**—**Id(4)** showed monomodal SEC curves that shifted toward lower values along the retention time scale as the molar ratio R increased (Figure 3).
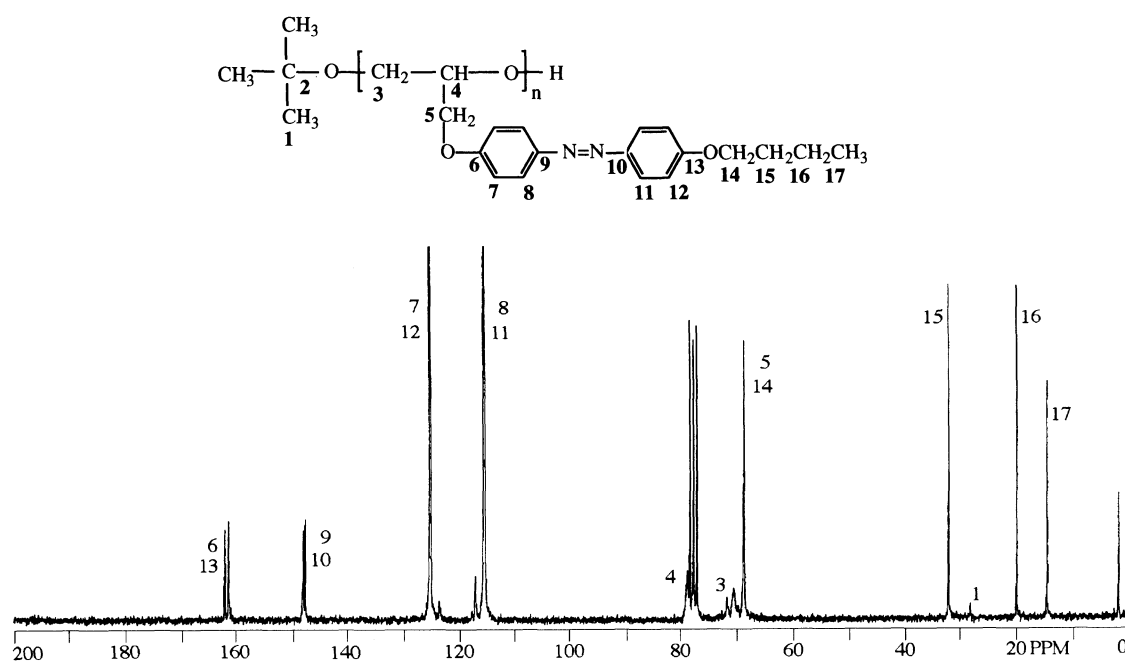
Scheme 1.

Figure 1. ^{13}C NMR spectrum in CDCl$_3$ of polymer **Id(4)**.

Table I. Concentration data, yields and molar mass characteristics of polymers Ia—Ig

Sample	m	$[M_0]/mol\,L^{-1}$	$R = [M_0]/[I_0]$	Yield/%	$M_n{}^a$	$M_w/M_n{}^a$	$M_n{}^b$
Ia	0	0.23	20	25	3500	1.15	7500
Ib	1	0.18	20	30	4500	1.12	8000
Ic	2	0.21	20	45	4500	1.14	—[c]
Id(1)	3	0.13	5	65	3200	1.14	5500
Id(2)	3	0.16	10	40	3700	1.11	9500
Id(3)	3	0.16	20	30	4200	1.12	12000
Id(4)	3	0.16	30	30	5700	1.12	14500
Ie	4	0.20	20	40	4800	1.15	13000
If	5	0.15	20	25	3900	1.12	9000
Ig	9	0.16	20	45	5700	1.10	—[c]

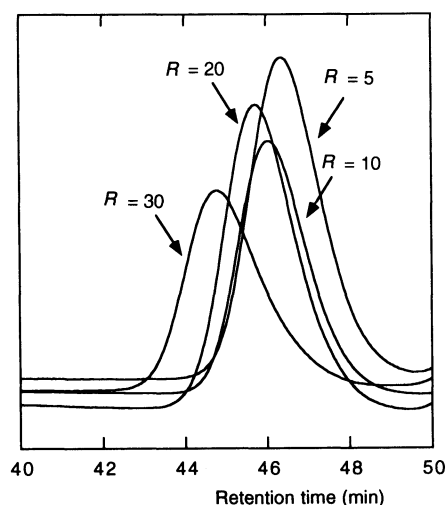[a] By SEC (CHCl$_3$, 25°C). [b] By ^{1}H NMR. [c] Not determinable.
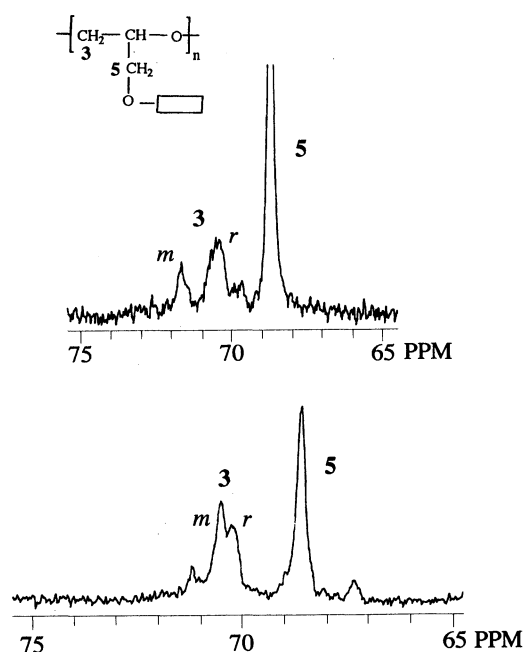
Figure 2. ^{13}C NMR spectra in the 75—65 ppm region of polymers Id(4) (top) and IIb(7) (bottom). (Rectangle indicates aromatic core.)

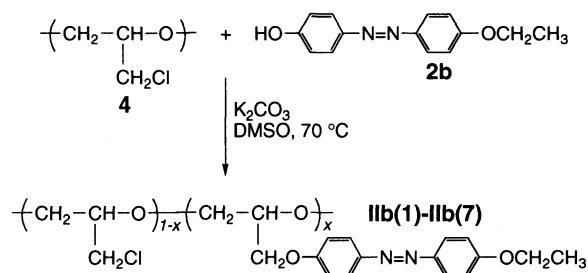Figure 3. SEC curves of polymers Id(1)—Id(4) prepared with different molar ratios R.

Polymers IIb(1)—IIb(7) were prepared by a grafting reaction of 4-hydroxy-4'-ethoxy-azobenzene onto preformed poly(epichlorohydrin) (4) (Scheme 2). The modification reaction was carried out in anhydrous dimethyl sulfoxide at 70°C with anhydrous potassium carbonate in the presence of benzyltributylammonium bromide. Different reaction times were used for the grafting, and accordingly the polymer samples exhibited different degrees of substitution ranging from 24 to 80% (Table II). A content of about 60% of dyads m was evaluated for each polymer sample consistent with a slightly predominant isotactic character[13] (Figure 2). The SEC values of M_n and M_w/M_n were around 100000 and 3.7, respectively, thus indicating that the grafting reaction did not degrade the polymer backbone in a substantial way. However, higher reaction temperatures resulted in a partial backbone degradation of the parent polymer 4.

Liquid Crystalline Behavior

The phase transition temperatures of monomers 3a— 3g, polymers Ia—Ig, and IIb(1)—IIb(7) were determined by DSC measurements and/or polarizing mi-

Scheme 2.

Table II. Molecular characteristics and liquid crystal properties[a] of polymers IIb(1)—IIb(7)

Sample	Grafting[b] %	$M_n{}^c$	$M_w{}^c / M_n$	T_{I-N} K	$T_{N-S_{A2}}{}^d$ K	ΔH_{I-N} $J\,g^{-1}$
IIb(1)	24	95000	3.6	—[e]	—	—
IIb(2)	40	95000	3.8	—[e]	—	—
IIb(3)	55	95000	3.8	399	—	4.1
IIb(4)	70	100000	3.7	434	—	3.7
IIb(5)	73	100000	3.7	441	421	3.5
IIb(6)	75	100000	3.8	450	435	3.8
IIb(7)	80	110000	4.0	458	444	4.4

[a] By DSC, at 10 K min^{-1} scanning rate. [b] By ^{1}H NMR. [c] By SEC. [d] By optical microscopy. Enthalpy not detected by DSC. [e] Not liquid crystalline.

Table III. Phase transitions parameters[a]
of monomers 3a—3g

Sample	m	$T_{\mathrm{m}}/\mathrm{K}$	$T_{\mathrm{I-N}}/\mathrm{K}$	$\Delta H_{\mathrm{I-N}}/\mathrm{J\,g^{-1}}$
3a	0	399	(387)	2.3
3b	1	431	(409)	4.0
3c	2	427	—	—
3d	3	402	(395)	3.3
3e	4	387	(384)	3.0
3f	5	386	391	2.5
3g	9	380	(377)	3.7

[a] Melting (m) and isotropic–nematic (I–N) transitions, by DSC at $10\,\mathrm{K\,min^{-1}}$ scanning rate. Monotropic transitions in parentheses.
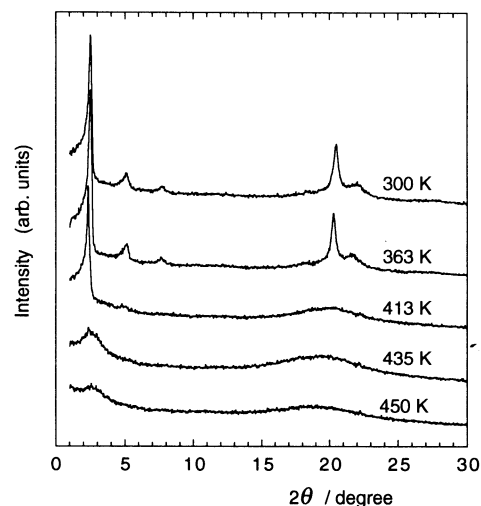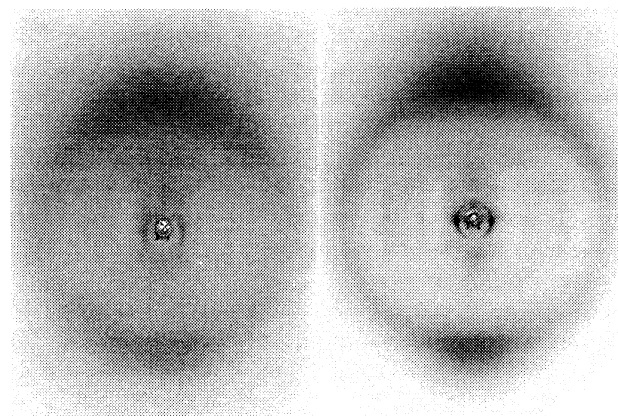
Table IV. Phase transition temperatures and enthalpies
(in $\mathrm{J\,g^{-1}}$, in parentheses) of polymers Ia—Ig on cooling
at $10\,\mathrm{K\,min^{-1}}$ scanning rate (some enthalpies
not detected by DSC)[a]

$$\textbf{Ia:} \quad I \xrightarrow[(4.1)]{440\,\mathrm{K}} N \xrightarrow{432\,\mathrm{K}} S_{A2}$$

$$\textbf{Ib:} \quad I \xrightarrow[(4.4)]{466\,\mathrm{K}} N \xrightarrow{413\,\mathrm{K}} S_{A2}$$

$$\textbf{Ic:} \quad I \xrightarrow[(3.3)]{444\,\mathrm{K}} S_{A2} \xrightarrow{393\,\mathrm{K}} S_{X}$$

$$\textbf{Id(3):} \quad I \xrightarrow[(4.7)]{466\,\mathrm{K}} N \xrightarrow{426\,\mathrm{K}} S_{A2} \xrightarrow[(14.2)]{399\,\mathrm{K}} S_{X}$$

$$\textbf{Ie:} \quad I \xrightarrow[(8.8)]{488\,\mathrm{K}} S_{C2} \xrightarrow[(19.0)]{407\,\mathrm{K}} S_{X}$$

$$\textbf{If:} \quad I \xrightarrow[(9.7)]{448\,\mathrm{K}} S_{C2} \xrightarrow[(12.3)]{392\,\mathrm{K}} S_{X}$$

$$\textbf{Ig:} \quad I \xrightarrow[(11.2)]{470\,\mathrm{K}} S_{Ad} \xrightarrow[(9.4)]{377\,\mathrm{K}} S_{X}$$

[a] See the text for symbols.

Figure 4. X-Ray powder diffraction spectra of polymer **Id(3)** in different phases: 300 K (virgin sample); 363 K (unidentified ordered smectic); 413 K (smectic S_{A2}); 435 K (nematic); 450 K (isotropic).

Figure 5. X-Ray diffraction pattern of magnetically aligned polymer **Ia** in the nematic phase at 434 K (left) and in the smectic phase at 300 K (right) (horizontal direction of the magnetic field).

croscopy. The nature of the LC phases was identified by qualitative observations of the optical textures and by X-ray diffraction. The LC properties of the monomers 3a—3g are summarized in Table III. 3a—3b and 3d—3f formed a nematic mesophase which was enantiotropic for 3f only. No mesophase was observed for 3c.

The glass transition temperature (T_{g}) of polymers Ia—Ig was difficult to detect but seemed to be essentially unaffected by the repeat unit structure, *i.e.*, it was 330 K for Ia, 343 for Ib, and 333 K for Id(1). By constrast, their LC behavior depended significantly on the length of the terminal n-alkoxy tail (Table IV). Ia to Id containing short terminal tails $(m \leq 3)$ formed, with the exception of Ic, a nematic (N) and a bilayer smectic A (S_{A2}) mesophase. Ic presented an S_{A2} phase of comparatively great thermal stability, which transformed directly to the isotropic liquid (I) thereby inhibiting the formation of the N phase. Further lengthening the n-alkoxy tail $(m > 3)$ stabilized the packing of the side-chain mesogens in Ie to Ig, that were purely smectic. However, accommodation of the expanded side-chain mesogens in smectic layers was realized either by a tilt of the molecules in a bilayer smectic C (S_{C2}) structure in Ie and If, or by a partial overlap of the molecules in an interdigitated smectic A (S_{Ad}) structure in Ig. Polymers Ic to Ig formed an additional ordered smectic (S_{X}) mesophase, the nature of which could not be unequivocally identified.

The evolution with temperature of the mesophases was studied by X-ray diffraction and is illustrated here for Id(3) (Figure 4). On cooling from the isotropic liquid, an I–N phase transition was first observed at 446 K, as evidenced by the strengthening of the low-angle diffuse signal at about $2\theta \approx 2.5°$ associated with the short-range positional order of the side-chain groups. A further temperature decrease below 426 K resulted in the occurrence of a disordered smectic mesophase with a layer thickness $d = 35.5\,\text{Å}$ and an average intermolecular distance within the liquid-like layers $D \approx 4.5\,\text{Å}$. Comparison of the measured value of d with the length L of the side-group mesogens in their fully extended conformation, $L = 19.5\,\text{Å}$, suggests the existence of an S_{A2} phase. The X-ray diffraction pattern below 399 K presented three Bragg peaks in the low-angle region (with spacings in the ratio 1 : 2 : 3), associated with a correlated lamellar structure with $d = 36\,\text{Å}$, and two to three sharp peaks localized in the wide-angle region typical of an ordered smectic mesophase S_{X}. These findings were confirmed by X-ray diffraction investigations on magnetically aligned polymer samples. The polymers were aligned by slowly cooling from the isotropic liquid to the desired temperature under the magnetic field, as typified here for

**Table V.** Liquid crystalline properties[a] of polymers
Id(n) (m = 3).

Sample	T_{I-N}	$T_{N-S_{A2}}$[b]	$T_{S_{A2}-S_X}$	ΔH_{I-N}	$\Delta H_{S_{A2}-S_X}$
	K	K	K	$J g^{-1}$	$J g^{-1}$
Id(1)	432	395	376	3.1	5.5
Id(2)	442	415	392	3.6	10.0
Id(3)	446	426	399	4.7	14.2
Id(4)	455	433	411	8.7	25.0

[a] By DSC, on cooling at $10 \, K \, min^{-1}$ scanning rate. [b] By optical microscopy.

Ia. The nematic phase resulted to be rather well aligned, with the side-chains being oriented nearly parallel to the magnetic field (Figure 5). On approaching the nematic–smectic transition from higher temperature, diffraction signals appeared in the low-angle region due to nematic cybotactic groups in a pre-transitional state. In the smectic phase, the layer Bragg reflections occurred on the meridian, thus indicating that the smectic layers were perpendicular to the magnetic field direction (Figure 5). The two diffuse crescents on the equator in the wide-angle pattern proved the formation of a disordered smectic phase with the mesogenic side chains being oriented orthogonal to the smectic layer planes. Annealing treatments of the aligned sample at temperatures slightly higher than ambient temperature induced partial crystallization. A detailed X-ray diffraction study on oriented samples is in progress to identify the exact structure of the smectic mesophases and will be reported in a forthcoming paper.

The effects of varying M_n of the polymer samples on the phase transition parameters were analyzed for **Id(1)**—**Id(4)** that gave rise to three different mesophases (Table V). The trends with M_n of the S_X–S_{A2}, S_{A2}–N, and N–I transition temperatures and enthalpies are shown in Figures 6 and 7, respectively. The LC phase transition temperatures increased regularly with increasing M_n and, in a parallel fashion, the enthalpy changes associated with the LC transitions followed the same ascending trend. This behavior of the phase transition parameters with M_n is in general agreement with that found for other polymeric systems,[13,14] although the degree of polymerization above which the phase transition parameters become independent of M_n seemed not to have been reached yet.

Samples **IIb(1)**—**IIb(7)** were not crystalline, but T_g was only detected in **IIb(7)** at 335 K. The LC properties were strongly correlated with the percent grafting of mesogenic side chains (Table II). **IIb(1)** and **IIb(2)** incorporating small amounts (< 50%) of mesogenic side chains did not form any LC mesophase. **IIb(3)** and **IIb(4)** containing intermediate amounts (≤ 70%) of mesogenic side chains were nematic, whereas **IIb(5)** to **IIb(7)** incorporating greater contents of mesogenic units presented both N and S_{A2} mesophases. In no case was the S_{A2}–N temperature detected by DSC, probably because this phase transition extended over a wide temperature range with a low enthalpy associated with it. There was a minimum substitution limit of approximately 50% necessary for a liquid crystal phase to be formed, consistent with literature data.[5] Furthermore, the transition temperatures increased with increasing amount of mesogenic
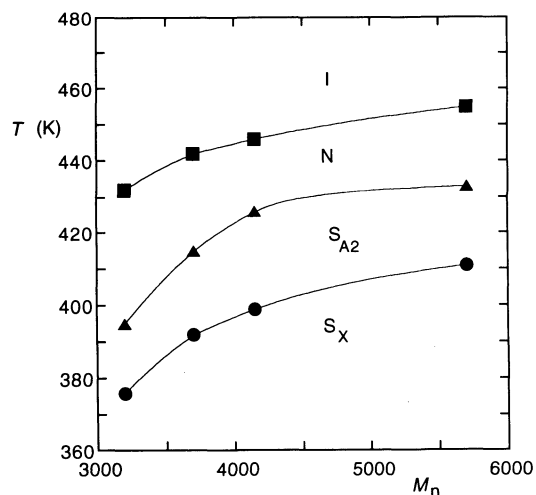
Figure 6. Trends of the I–N (■), N–S_{A2} (▲), and S_{A2}–S_X (●) transition temperatures of polymers **Id(1)**—**Id(4)** as a function of the SEC molar mass.
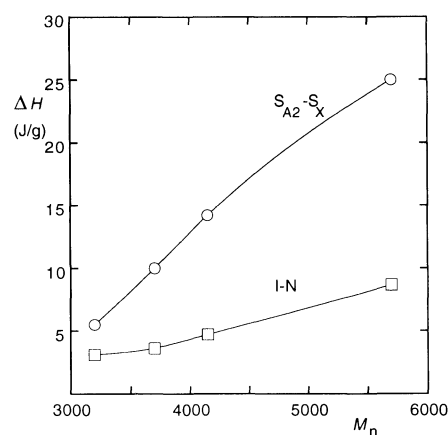
Figure 7. Trends of the I–N (□) and S_{A2}–S_X (○) transition enthalpies of polymers **Id(1)**—**Id(4)** as a function of the SEC molar mass.

units in the polymer. However, while the value of the N–I temperature tended to that detected for the corresponding **Ib**, the value of the S_{A2}–N temperature was much higher than for **Ib**. It appears that the residual unsubstituted side chains did not disfavor smectic ordering but rather increased the flexibility of the polymer backbone, thereby improving the ability of the mesogenic groups to arrange in a more effective space filling manner. This could also be enhanced by the prevalently isotactic character of this class of polymers.

CONCLUSIONS

Poly(glycidyl ether)s **Ia**—**Ig** were synthesized by ring-opening anionic polymerization of mesogenic epoxides. They presented relatively low molar masses and narrow molar mass dispersities. Their liquid crystal behavior included smectic–nematic or smectic–smectic sequences of mesophases, strongly depending on the length of the terminal tail on the mesogenic side chain. The trend of the phase transition parameters with molar mass suggested that mesophases of the same kind would also form in samples with greater molar masses. Poly(glycidyl ether)s **IIb(1)**—**IIb(7)**, that compare with **Ib**

918

Polym. J., Vol. 31, No. 11-1, 1999

in terms of chemical structure, were prepared by a polymer-analogous modification of a preformed polymer. This procedure permitted obtaining samples differing in the degree of side-chain substitution over a significant range. The formation of liquid crystal mesophases brought about by the lateral interaction of the mesogenic side chains depended on the amount of unsubstituted residues that influenced the degree of order. Therefore, nematic mesophases were only obtained for degrees of substitution greater than 50%, while further, smectic mesophases were detected for samples with more than 70% mesogenic side chains.

In no smectic polymer was a monolayer structure found. This is in agreement with the observation that the arrangement in monolayers on the one hand or in bilayers on the other hand depends on the conditions to realize a space filling dense packing, especially the steric hindrance of antiparallel arrangement of side chains within monolayers due to the spacer to tail length ratio.[15] The lack of a spacer segment in the poly(glycidyl ether)s essentially favored bilayer structuring in the smectic mesophases.

REFERENCES

1. C. B. Mc Ardle, Ed., "Side-Chain Liquid Crystal Polymers," Blackie, Glasgow, 1989.
2. V. P. Shibaev and N. A. Platé, *Polym. Sci. USSR*, **19**, 1065 (1977).
3. V. P. Shibaev and N. A. Platé, *Adv. Polym. Sci.*, **60/61**, 173 (1984).
4. C. Pugh and V. Percec, *Polym. Bull. (Berlin)*, **16**, 521 (1986).
5. S. Piercourt, N. Lacoundre, A. Le Borgne, N. Spassky, C. Friederich, and C. Noel, *Makromol. Chem.*, **193**, 705 (1992).
6. (a) E. Akiyama, Y. Nagase, and N. Koide, *Makromol. Chem., Rapid Commun.*, **14**, 251 (1993); (b) E. Akiyama, M. Ohtomo, Y. Nagase, and N. Koide, *Macromol. Chem. Phys.*, **196**, 3391 (1995).
7. D. Taton, A. Le Borgne, N. Spassky, and C. Noel, *Makromol. Chem.*, **196**, 2941 (1995).
8. A. S. Angeloni, D. Caretti, C. Carlini, E. Chiellini, G. Galli, A. Altomare, R. Solaro, and M. Laus, *Liq. Cryst.*, **4**, 513 (1989).
9. F. Schmidt and E. Bayer, in "Methoden der Organischen Chemie (Houben-Weyl)," B.VI/2, Saurstoffverbindungen I, Vierte Auflage, G. Thieme Verlag, Stuttgart, 1963, p 9.
10. A. Stolarzewicz, *Makromol. Chem.*, **187**, 745 (1986).
11. H. Koinuma, K. Naito, and H. Hirai, *Makromol. Chem.*, **183**, 1383 (1992).
12. J. C. Ronda, A. Serra, A. Mantecon, and V. Cadiz, *Polymer*, **36**, 471 (1995).
13. H. Stevens, G. Rehage, and H. Finkelmann, *Macromolecules*, **14**, 1543 (1984).
14. V. Percec, D. Tomazos, and C. Pugh, *Macromolecules*, **22**, 3259 (1989).
15. D. Wolff, *SPIE Proc.*, **2**, 2651 (1996).

Polym. J., Vol. 31, No. 11-1, 1999

919